Al-Azhar University Civil Engineering Research Magazine (CERM)
Vol. (43) No. (2) April . 2021

Nonlinear Analysis of Reinforced Concrete T-Beam

Osman M. O. Ramadan[a], Ahmed H. Abdel-Kareem[b], Hala R. Abou safa[b], and Ibrahim A. El-Azab[b]*

[a]Department of Civil Engineering, Cairo University, Cairo, Egypt
[b]Department of Civil Engineering, Benha University, Benha, Egypt

الملخص العربى :

تستخدم الكمرات الخرسانية المسلحة ذات الشفه علي نطاق واسع في مجال الهندسة المدنية، حيث أنها تستخدم في العديد من المنشأت والتطبيقات والعناصر الخرسانية. تم عمل العديد من الدراسات العملية والنظرية علي هذا النوع من الكمرات وقد اثبتت أهميتها في مقاومة قوي القص بشكل فعال. في هذا البحث نقوم بعمل التحليل النظري باستخدام نظرية العنصر المحدود من خلال استخدام برنامج " ANSYS " وكذلك دراسة متغيرات جديده بعد التحقق من النموذج النظري للكمرات الخرسانية المسلحة ذات الشفة وتأثير الشفة علي مقاومة قوي القص من خلال عمل نماذج لبعض العينات التي تم اختبارها بالفعل ومقارنة النتائج لها للتأكد من صحة النموذج المستخدم، كما أنه تم دراسة متغيرات جديدة بواسطة النموذج المشار له، ومن هذه المتغيرات دراسة مقاومة الخرسانة، نسبة أبعاد الشفة الخرسانية من حيث العمق والعرض لها لأبعاد العصب ، النسبة بين بحر القص وعمق العينة، و أخيرا نسبة الحديد الطولي بالشفة.

Abstract:

The main objective of this research is to study the shear strength outcomes from the nonlinear constitutive reinforced concrete T-beam models and make a comparison with experimental results. The models were performed in the finite element computer program ANSYS V-19.2 so as to apply the 3D nonlinear analysis of flanged specimens. Ninety-six samples were tested simply supports under two concentrated points of static loading up to failure. Several validation studies have been carried out on flanged beams with variable flange dimensions. The current work presents good results between experimental and numerical results about (1.03 and 0.87 %) for the load-deflection curves and the crack patterns. Moreover, parametric studies have been occurred to discuss the effect of structural parameters on the performance of T-section against shear straining action. Four design parameters were arranged to involve flange dimensions, longitudinal reinforcement in flange, concrete compressive strength “fc”, and shear span to depth ratio. Beams were shown to obtain the load-deflection relationships, the ultimate loads, and the crack patterns. Therefore, they are compared to the solid reference one. The flange dimensions effect on the increased the shear strength by up to 260% of the shear strength of the web alone, and the effect of longitudinal reinforcement in flange enhancements the shear capacity up to 40%, finally shear span to depth ratio improvements the shear strength from 85%

to 260%. Three experimental T-beams were in the main concern of this research and they were done in variety to ensure the validity of types.

Keywords: finite element analysis, shear strength, reinforced concrete beams, T-beam, Girder

1. Introduction

Flanged reinforced concrete beams have been widely used in many applications in the field of civil engineering. The attitude of this kind of structural members was discussed experimentally as well as analytically. Numerical analysis technique that is based on the finite element method has been checked in this research to detect the effect of the flange on the reinforced concrete T-beam in both pre- and post-cracking stages of loading and up to ultimate load.

ANSYS [1] is one of the most exceedingly famous computer programs which used structural analysis through the finite element method. The overall study in the area of numerical modeling and finite element supports the engineers and researchers with many applications not only in construction on but also in other industries and scientific aspects. One of the characteristics of ANSYS, which was appealing to researchers, is the possibility of specification through adding extra features and qualities. This simplified the research process by contributing in the production of new material models or finite elements and anticipated to the spread of understanding knowledge in all scientific realms.

According to Hesham et al. [2] a numerical experimental study was fulfilled to check the validity of using lightweight concrete beams. It observed the shear behavior of lightweight concrete; six lightweight concrete beams were tested in two-point bending to urge the effect of flange width and shear span on depth ratio. In the experimental and FE studies, the failure load of the T-beams with different flange widths (320, 520, and 720 mm) were increased in proportion to the flange width. During the experimental and FE studies, the failure load noticed to be inversely proportional to all the shear span to depth ratio, vertical deflection, longitudinal steel strain, stirrup steel strain, and compressive concrete strain of the T-beams with various flange widths (320, 520, and 720 mm) respectively.

As Balamuralikrishnan et al. [3] mentioned, the main objective of this work is to evaluate the static load trend of RC T-beams reinforced internally with GFRP reinforcements using finite element analysis software ANSYS. Totally twelve numbers of specimens were completely Pm outlined in this study in a way of varying parameters such as the type of reinforcements, reinforcements ratio, and concrete grade. Modeling of the T- beams was done with ANSYS by using solid 65 and link 8 element and the same was tested under static loading atmospheres. The experimental outcomes of the flanged beams met perfectly that of the analytical results that were gathered from the flanged beams reinforced with steel and GFRP reinforcements.

2. Finite Element Modeling Using ANSYS

2.1. Geometric

Finite element modeling and nonlinear analysis are performed by using ANSYS software. The structural element types which helped for geometric idealization of the different materials

are SOLID 65 for concrete, LINK 8 for steel bars and stirrups. In order to avoid stress concentration problems such as localized crushing of concrete elements near the bearing and loading plates, steel plates with 30 mm thickness are modeled by SOLID 45 at the location of supports and loading places in specimen. The structural element types functioned to simulate the different materials which are presented in Fig. 1. For solving the nonlinear analysis equations of specimen, Newton- Raphson equilibrium iteration technique is used in the ANSYS software. This technique relayed on a series of successive linear approximations with corrections. According to this study, the convergence criterion relies on a displacement control. The infinite norm of displacement and the convergence precision is 0.05 [9,10,11]. Thus, to improve the convergence of nonlinear analysis, adaptive descend gene, linear searching, fore-casting, and dichotomy were applied at the same time. The displacement boundary conditions are necessary to protect the models. To show the cut off support boundary condition of the specimen, the translations at the nodes (UX, UY and UZ) were specified as a constant value of zero, whereas the other support was displayed as roller by indicating the translations at the nodes (UY) equal zero value. The force (P) at two points was placed at the top of specimen in the gravity direction to reveal the experimentally tested. The applicable load was known as incremental loads. There was an adjustment for every increase in the result at certain specific load level. Fig. 2 shows the occurred load and the supports conditions. The maximum number of iterations in each load step was set as program default.

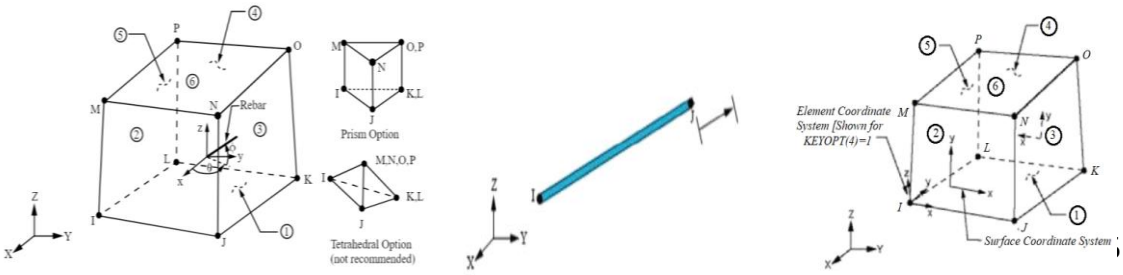

Fig. 1. Structural elements idealization for the numerical models [9]

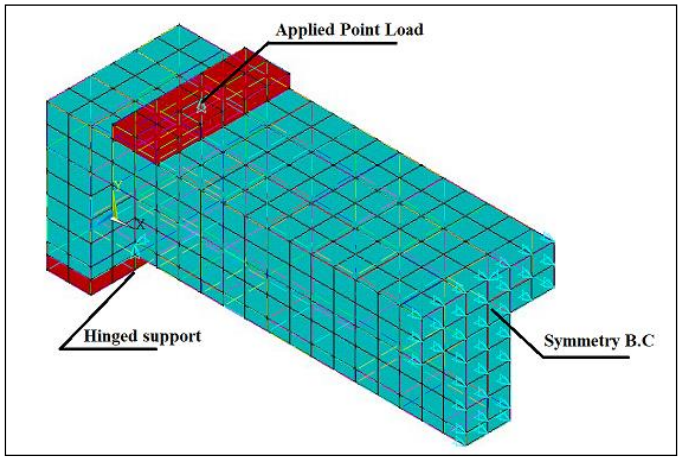

Fig. 2. Applied Load and Support Conditions.

2.2. Constitutive Relations

Constitutive relationships were desired to connect average stresses to average strains for both the reinforcement as well as the concrete. These relations may deviate much from the usual local stress-local strain relations which are specified by the standard materials tests.

2.2.1. Constitutive relation for concrete

To develop a model for the attitude of concrete, it was a difficult activity. Concrete is a quasi-brittle material and has different reaction in compression and tension. The tensile strength of concrete is typically 8-15% of the compressive strength [12](*Shah, et al. 1995*). Fig.3 shows a typical stress-strain curve for normal weight concrete [13](*Bangash 1989*).

To cover a descriptive analysis, the stress-strain curve expressed for concrete is linearly elastic up to about 30 percent of the maximum compressive strength. Above this point, an increase of stress is shown gradually up to the maximum compressive strength. After it reaches the maximum compressive strength f_{cu}, the curve begins to decline into a softening region. finally, crushing failure happens at an ultimate strain ε_{cu} .

In tension, the stress-strain curve for concrete is almost linearly elastic up to the maximum tensile strength. After this point, the concrete cracks and the strength rises down gradually to zero [13].

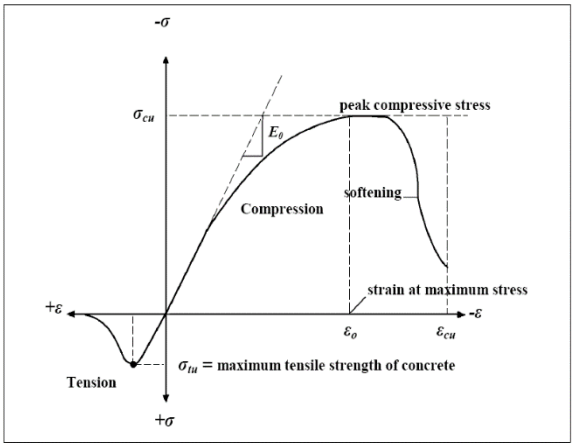

Fig. 3. Typical uniaxial compressive and tensile stress-strain curve for concrete (*Bangash 1989*)

For concrete, ANSYS requires input data for qualifications of materials as follows:

Elastic modulus (E_c).

Ultimate uniaxial compressive strength (f'_c).

Ultimate uniaxial tensile strength (modulus of rupture, f_r).

Poisson's ratio (v).

Shear transfer coefficient (β_t).

2.2.1.1. Compressive Uniaxial Stress-Strain Relationship for Concrete

The uniaxial stress-strain relationship for concrete in compression was needed to the ANSYS program. Numerical terminologies (*Desayi and Krishnan 1964*), Eq. 1 &2, were used along with Eq.3 (*Gere and Timoshenko 1997*) to establish the uniaxial compressive stress-strain curve **for concrete [14].**

$$f = \frac{E_c \varepsilon}{1 + \left(\frac{\varepsilon}{\varepsilon_0}\right)^2} \quad \textbf{(1)}$$

$$\varepsilon_0 = \frac{2 f'_c}{E_c} \quad \textbf{(2)}$$

$$E_c = \frac{f}{\varepsilon} \quad \textbf{(3)}$$

Where:

f = stress at any strain ε , psi

ε = strain at stress f

ε_o = strain at the ultimate compressive strength f_c'

E_c = the initial tangent modulus for concrete in MPa and is defined according to ACI-318 14 [17] by the following equations:

$$E_c = 4700\sqrt{f_c'} \quad (4)$$

Fig. 4 shows the simplified compressive uniaxial stress-strain relationship that was used in this study.

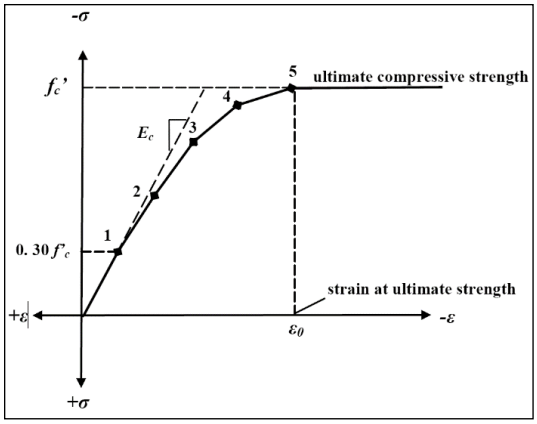

Fig. 4. Simplified compressive uniaxial stress-strain curve for concrete

The simplified curve of which reflects stress-strain for each beam model is formed from six points. The points are related by straight lines. The curve begins at zero stress and strain. Point No. 1, at 0.30f'_c, is calculated for the stress-strain relationship of the concrete in the linear range (Eq.3). Point Nos. 2, 3, and 4 are gained from (Eq.1), in which ε_0 is calculated from (Eq.2). Point No. 5 is at ε_0 and f_c'.

2.2.1.2. Failure *Criteria for Concrete*

The model gives an expect failure for concrete materials. The cause for this return to both cracking and crushing failure modes. The two input strength parameters *i.e.*, ultimate uniaxial tensile and compressive strengths are important to define a failure surface for the concrete. Then, the standard of concrete failure DC which is caused by a multi-axial stress state can be calculated (*William and Warnke 1975*). A three-dimensional failure surface for concrete is described in Fig.5. The most considerable nonzero principal stresses found in the x and y directions, are symbolized by σ_{xp} and σ_{yp}, respectively. Three failure in the surfaces are exhibited as projections on the σ_{xp}-σ_{yp} plane. The mode of failure is a function of the sign of σ_{zp} (principal stress in the z direction).

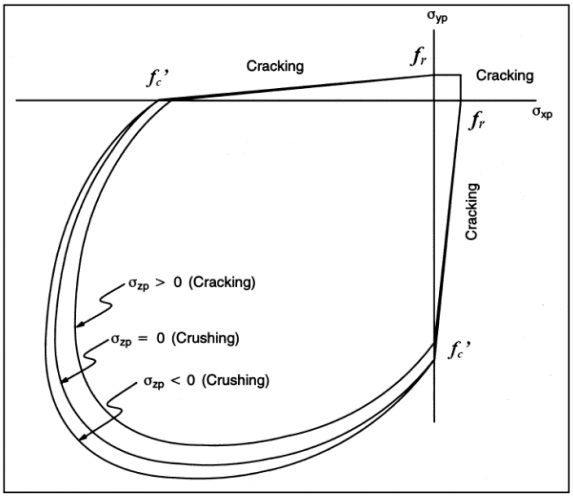

Fig.5. 3-D failure surface for concrete (*ANSYS*)

For example, if σ_{xp} and σ_{yp} are both negative (compressive) and σ_{zp} is slightly positive (tensile), cracking would be revealed in a direction perpendicular to σ_{zp} Although, if σ_{zp} is zero or slightly negative, it is supposed that the material will crush.

2.2.2. Constitutive relation for steel

The experimental beams originated steel reinforcement with typical Grade 60 steel reinforcing bars. In this FEM discussion, steel reinforcement had certain qualities, i.e., elastic modulus and yield stress, it follows the design material properties shown in the experimental investigation (*Kachlakev and McCurry 2000*). The steel for the finite element models was assumed to be an elastic-typical plastic material and identical in tension and compression. Poisson's ratio of 0.3 was applied for the steel reinforcement in this study (*Gere and Timoshenko 1997*). Fig.6 shows the idealized stress-strain relationship mentioned in this research. Material properties for the steel reinforcement are stated as follows:

Elastic modulus, E_s = 200,000 MPa

Yield stress, f_y = 420 MPa (Lab test)

Poisson's ratio, v = 0.3

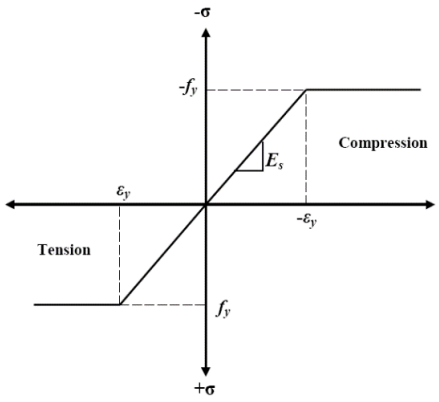

Fig.6. Idealized stress-strain curve for reinforcing steel

3. Model Validation studies

Validation studies were discussed on several T-beams. Table 1 introduces a summary for the geometrical and mechanical properties of the available specimens. FE model offers an alternative tool that is used in the analysis process, and also for getting different results with the previously done experiments, Ahmed H. et al. [16]. The details and set-up of tested specimens are shown in shape. 7& 8 respectively. Also, the finite element simulation models are shown in Fig. 9

.

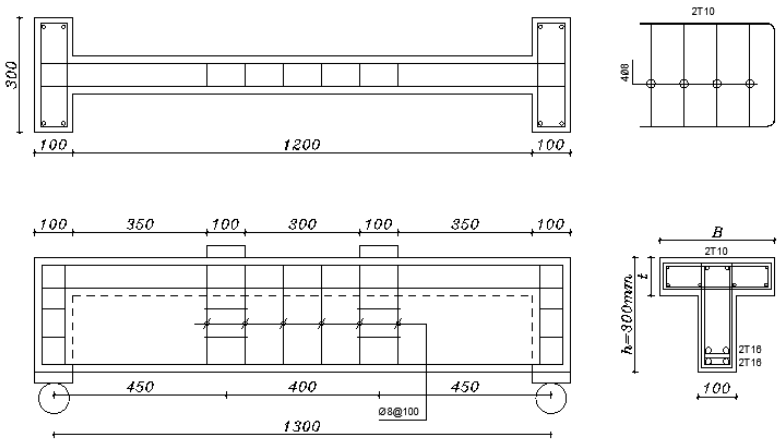

Fig. 7. Specimen details and arrangement of reinforcement (All dimensions in mm) [16]

[Table-1] Experimental Program

Specimen	Cross Sectional Area (cm^2)	Cross Sectional Area Increasing (%)	Flange Dim.			Stirrups in flange within shear zone (mm)	Longitudinal reinforcement in Flange		Longitudinal reinforcement in Flange [%]
			t_f (cm)	b_f (cm)	A_f (cm^2)		Bottom Steel	Top Steel	
C0	300	------			------	------		------	------
G1-T1-0.3	480	60%	0.3h= 9	30	270	------		------	------
G3-T3-0.5	900	200%	0.5h=15	50	750	Ø8@75	6 Ø 10 + 1Ø10/side	2 Ø 8 + 2 Ø 6	1.046%

G = Reinforcement group, "G1" without reinforcement, "G3" with longitudinal and stirrups in shear zone. Total depth 300 mm, web width (bw) 100 mm. T = Flange thickness, "T1=0.3h" 90 mm, "T2=0.4h" 120mm& "T3=0.5h" 150mm. 0.3&0.5 = Flange width; "0.3" 300 mm& "0.5" 500mm.

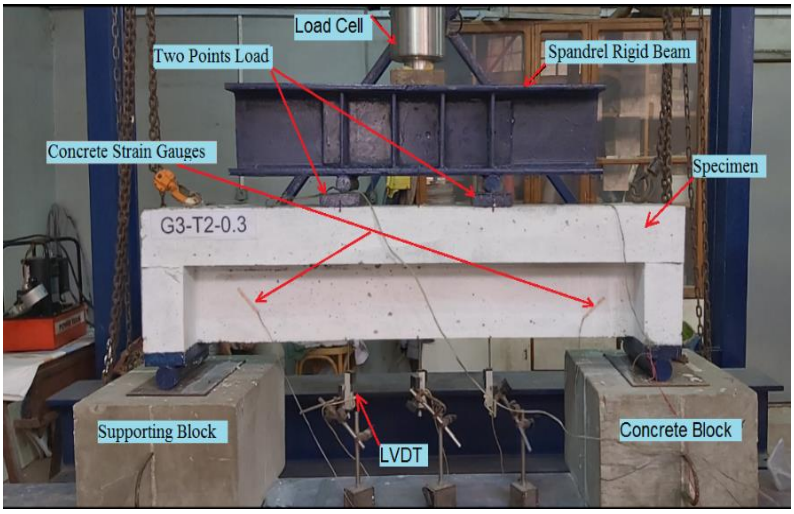

Fig. 8. Preparation of Test set-up Specimens [16]

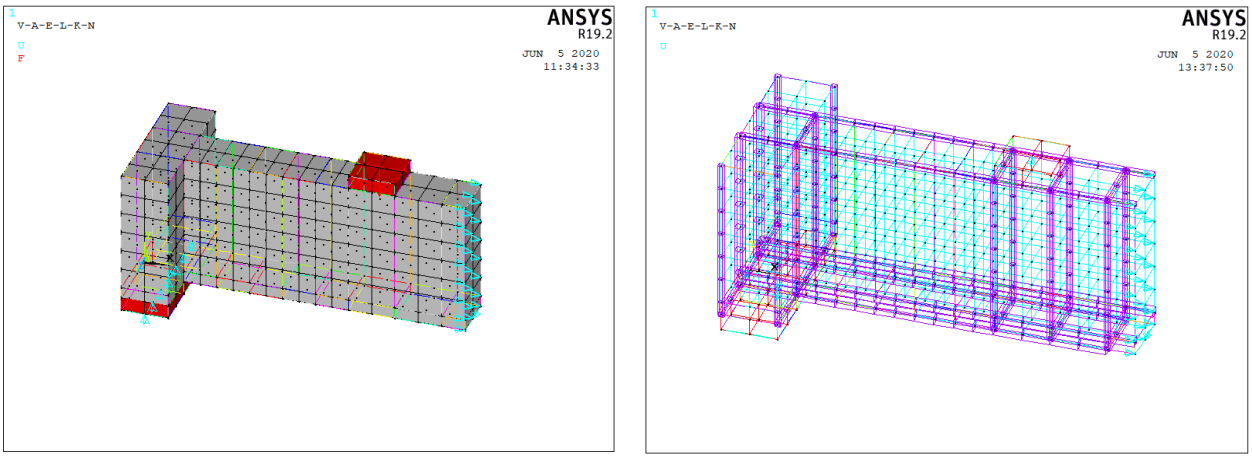

[a]- Finite Element Model for C0 (control)

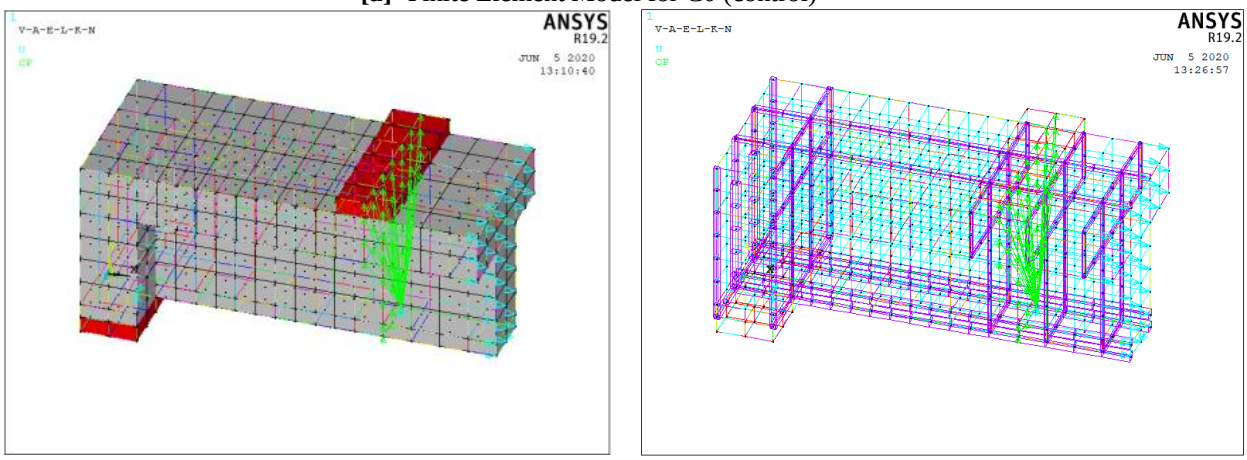

[b]- Finite Element Model for G1-T1-0.3

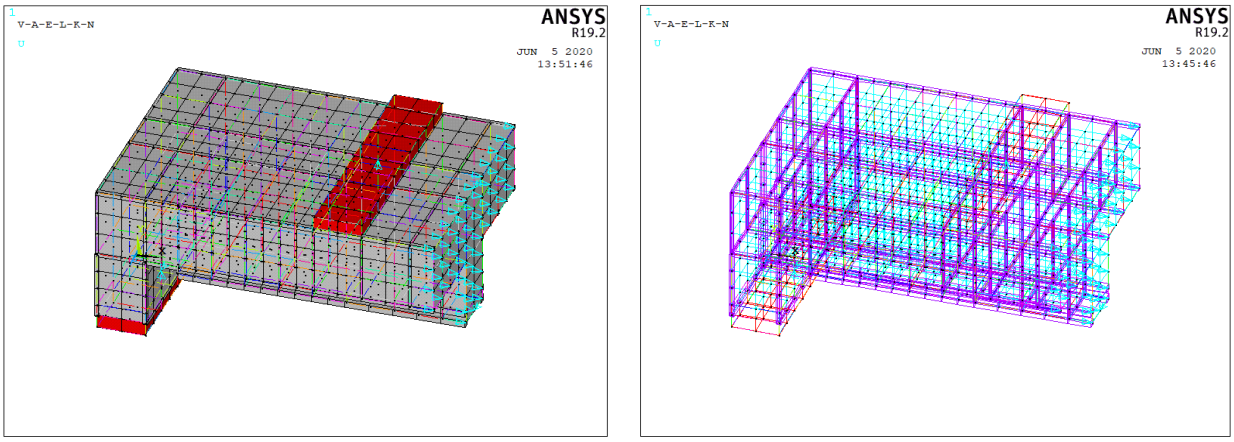

[c]- Finite Element Model for G3-T3-0.5

Fig. 9. Finite Element Simulation Models for specimens in Ref. [16]

3.1. Load deflection curves

The load-deflection curve achieved outlined results such as the ultimate load capacity (P_u) and the corresponding ultimate deflection (Δ_u). The area under the load-deflection curve which represents the toughness (I) is also calculated. Fig. 10 introduces the obtained numerical results altogether with the experimental results for definite specimens. The figure is reflecting a good agreement between the experimental results [16] and the desired results at different levels of response, the load-deflection plot from the finite element analysis matches well the experimental data for C0, G1-T1-0.3& G3-T3-0.5. In the linear range, the load-deflection which is derived from the finite element analysis is stiffer than that from the experimental results by about 10.7, 8.8& 16.1% respectively.

Fig. 10. Predicted and Measured Load-Deflections curves for specimens in Ref. [16]

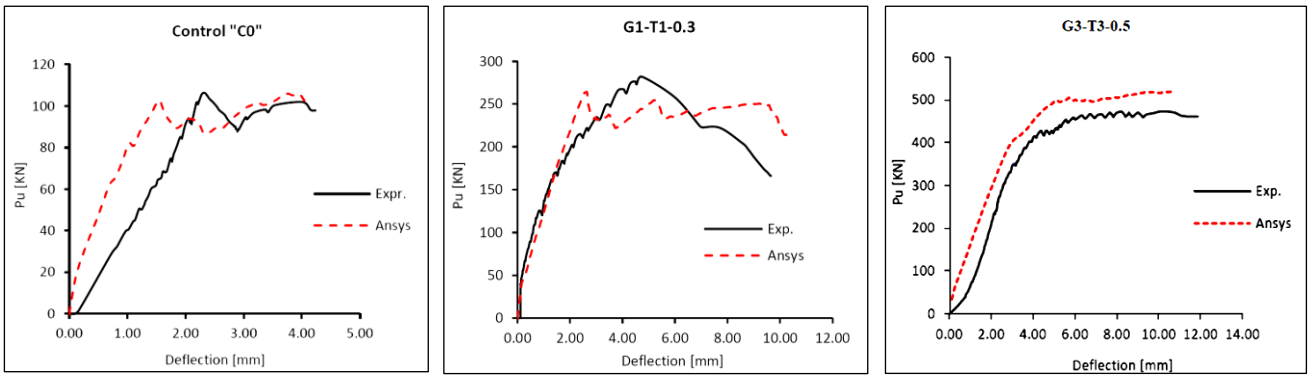

3.2. Ultimate load comparison

The ultimate load had the test for C0, G1-T1-0.3& G3-T3-0.5 was 106.4, 281.9& 473.8 kN respectively, while on the other hand the ultimate load obtained from ANSYS analysis was 113.4, 264.1& 516.2kN. So, the difference is about ± 6% and this assures that ANSYS program is an appropriate method to know the behavior of reinforced concrete T-beams.

3.3. Crack pattern and failure mode

A comparison between the predicted crack patterns against the experimental crack patterns for tested beams in Ref. [16] is shown in Fig. 11. As cleared in the shape, there is an outstanding harmonization noticed between the experimental and the numerical crack patterns. For all specimens suggested, the expected failure mode becomes shear mode. The failure mode is distinguished by wide shear diagonal cracks which occurs so close to the support column intersection with loading steel plate at the top. In addition, the figure describes that the spreading of cracks is changing in relation to the flange dimensions.

(a) Experimental crack pattern for C0 (b) Predicted crack pattern for C0

(c)Experimental crack pattern for G1-T1-0.3 (d) Predicted crack pattern for G1-T1-0.3

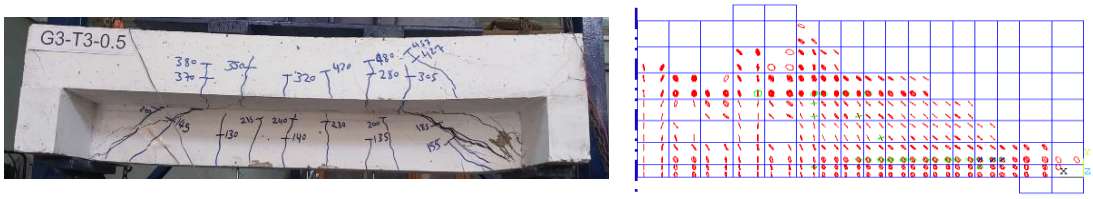

(e)

Experimental crack pattern for G3T3-0.5 (f) Predicted crack pattern for G3T3-0.5

Fig. 11. Predicted & observed cracking patterns for specimens in Ref. [16]

3.4. Concluding remarks

For all discussed cases, a noticed connection found due to the comparison between the experimental and the predicted results by finite element (FE) which involved the load-deflection curves and crack patterns. At the final level, the total average value for [$Pu_{(FE)}$ / $Pu_{(EXP)}$] ratio and [$\Delta u_{(FE)}$ /$\Delta u_{(EXP)}$] ratio for all specimens were 1.03 and 0.87 respectively. Hence, ANSYS computer program which was applied to joint with the offered constitutive models was a good tool for modeling. This program was mainly designed to study the flange effect on the shear strength of flanged reinforced concrete beam with or without longitudinal reinforcement in flange and with different material parameters.

4. Parametric study

4.1.General

Table 2 Parametric Study

Specimen	width ratio (ρ_b)	depth ratio (ρ_t)	*a/d*	$f_{c'}$	*Longitudinal steel in flange* ρ %	*No of Runs*
S	------	------	2.0	30	-----	1
S 01:12	3	0.10, 0.3, 0.5& 0.7	0.5, 1.0, and 2.0	30	0.5	12
					Total	13

Width ratio ($\rho_b = b_f/b_w$) is the ratio of flange width "b_f "and web width "b_w", depth ratio ($\rho_t = t/h$) is the ratio of flange thickness "t" and total web depth "h". Control specimen S is rectangular section, with total depth 300 mm and width 100 mm.

In order to discuss the effect of different parameters on the structural response; groups of reinforced concrete T-beam, which labeled as (S1, S2... S12) are analyzed. As given in Table 2, the main parameters studied here include: (1) the concrete strength (*fc'*), (2) width ratio (ρ_b), (3) depth ratio (ρ_t), (4) ratio of longitudinal steel in flange (ρ), and (5) shear span to depth ratio (*a/d*). For each parameter, the predicted response curve is personalized by the load-deflection curve. The control used specimen in this paper is the rectangular beam S plus the geometry given in Table 2.

4.2.Evaluation criteria of the parametric studies

The load - deflection curve gave an indication that the effects of the analyzed parameters, which have been already studied, are using the following measures:

- Loads at the yield level (P_y) and at the ultimate level (P_u).
- Deflection at the yield level (Δ_y) and at the ultimate level (Δ_u).
- Displacement ductility (μ_Δ) = (Δ_u/Δ_y).
- Toughness (I) = the area under the load-deflection curve.

For the above parameters, the outcomes of a specified specimen (S) are regarded as reference values to calculate the following relative measures:

$$Q_{uR}=P_u / P_{ur} \quad (5)$$

$$\alpha_{uR}=\Delta_u / \Delta_{ur} \quad (7)$$

$$I_{uR}=I / I_{ur} \quad (8)$$

Table 3 The output results for the analyzed specimens of parametric studies.

Specimen	P_u *(kN)*	P_y *(kN)*	P_{cr} *(kN)*	Δ_u *(mm)*	Δ_y *(mm)*	Δ_{cr} *(mm)*	Q_{uR}	α_{uR}	I	I_{uR}
S	141.61	------	33.47	2.81	------	0.34	1	1	1089	1.0
S1	559.50	356.40	140.44	2.86	3.03	0.36	3.95	1.02	2907	2.7
S2	516.96	437.77	142.56	2.04	2.51	0.33	3.65	0.73	3846	3.5
S3	692.85	430.30	150.87	2.91	3.18	0.38	4.89	1.04	3673	3.4
S4	714.67	N.Y*	178.62	2.43	N.Y*	0.38	5.05	0.86	4364	4.0
S5	300.22	210.57	72.36	2.53	2.82	0.38	2.12	0.90	1717	1.6
S6	328.58	271.78	72.66	2.67	3.53	0.33	2.32	0.95	2715	2.5
S7	440.19	427.09	73.28	3.92	4.21	0.34	3.11	1.40	3104	2.9
S8	500.99	N.Y	86.67	3.65	N.Y	0.33	3.54	1.30	3119	2.9
S9	156.09	100.52	38.30	2.69	7.35	0.32	1.10	0.96	1022	0.9
S10	198.57	147.53	35.73	3.57	5.05	0.27	1.40	1.27	1446	1.3
S11	270.99	195.03	37.47	4.50	5.37	0.27	1.91	1.60	1674	1.5
S12	354.17	N.Y	45.78	5.13	N.Y	0.29	2.50	1.83	2127	2.0

**: The longitudinal steel in flange Not Yield*

Where:

P_u : Ultimate load (kN).
P_y : Load at yielding of longitudinal steel reinforcement in flange (kN).
P_{cr} : Cracked load (kN).
Δ_u : The deflection at the ultimate (mm).
Δ_y : The deflection at the yielding (mm).
Δ_{cr} : The deflection at the first crack (mm).
I : The toughness (the area under the load-deflection curve).

Where:

Q_{uR} : Shear capacity ratio at the ultimate load level.
P_{ur} : Shear capacity at the ultimate load level for the control specimen (S).
α_{uR} : Deflection ratio at the ultimate load level.
Δ_{ur} : Deflection at the ultimate level for the control specimen.
I_{uR} : Toughness ratio.
I_{ur} : Toughness of the control specimen.

4.3. Effect of flange dimensions: width ratio ($\rho_b = b_f / b_w$) and depth ratio ($\rho_t = t/h$)

4.3.1. Width ratio (ρ_b)

A parametric thesis used the 3D FEM is implemented to convey the effect of flange dimensions (ρ_b & ρ_t) in T- beams on shear capacity. In the parametric investigation, the flange width was changed depending on width ratio ρ_b to shift from 3 to 9 as shown in table

2. Fig. 12 describes that predicted width ratio curve for four analytical T-beams. The result is compared to control beam S, they are all compared to flange width. The adequate providing main steel reinforcement causes all specimens to fail in shear failure mode. Then the Load increases step by step until the drop.

From the vivid shape it's found out that, beam with larger width ratio is showing higher ability in resisting shear capacity with reference to control beam. The shear capacity is rising up to 150, 209, 231& 262% respectively comparing to S specimen.

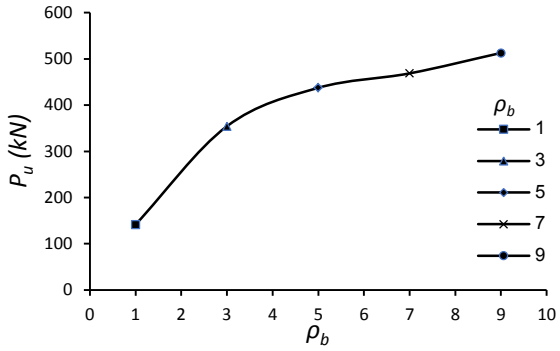

Fig. 12. Effect of flange width

4.3.2. Depth ratio (ρ_t)

The flange depth is changed according to depth ratio ρ_t that vary from 0.1 to 0.7 as shown in table 2. Fig. 13 reveals predicted depth ratio curve for four analytical T-beams, which is compared with control beam S. As shown in fig.13, a beam which has a larger depth ratio is showing higher ability in resisting shear capacity compared to S. The shear capacity is getting up gradually to 12.74, 75.13, 175.05, and 262.18% respectively comparing with S.

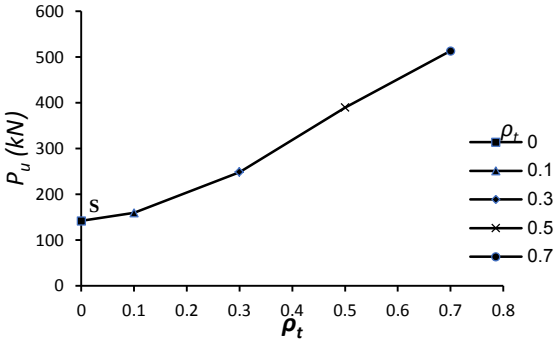

Fig. 13. Effect of flange depth

4.4. Effect of longitudinal steel in flange

The Three categories of longitudinal steel reinforcement ratio (ρ) in the flange occupy between 0.5, 1 and 2% in the flange concrete area. Fig.14 clarifies the comparison between the given results of some groups with deferent value of a/h. It indicates that when there is an increasing of ρ, it leads to a growth in shear capacity by 14:18% for a/h =0.5, 5:9 % for a/h = 1 and 37:40% for a/h = 2.

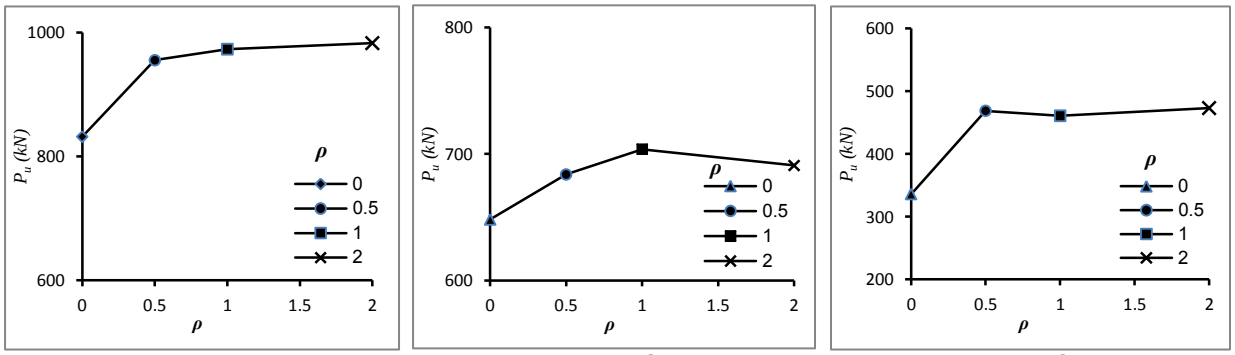

i. a/h = 0.5 *ii. a/h = 1* *iii. a/h = 2*

Fig. 14. Effect of longitudinal reinforcement in flange

4.5.Effect of shear span to depth ratio.

In this study three groups are explained with different shear span to depth ratio (*a/h*) "0.5, 1 and 2". The received results curves of a/h for the specimens with different flange width are involved in Fig. 14-(a&b). Mostly, an increase of (*a/h*) reduced the shear capacity of the flanged concrete beam. The decline of (*a/h*) ratio led to a good high rise in the shear capacity of flanged beam about 83:260 %. Fig.14-c represents the effect of (*a/h*) on the toughness, where the increasing (*a/h*)

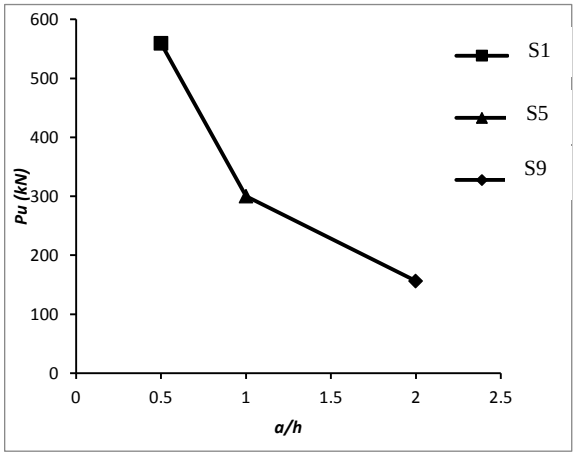

Fig. 14-a

decreases slightly the toughness (I). As shown in the load-deflection curves Fig.14-c, the toughness is lowered for example specimens S8& S12 when compared with S4 by 28% and 49% respectively.

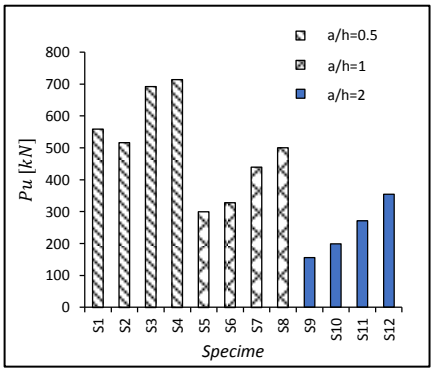

ρ = 0.5, ρb =3 & fcu = 30 MPa

Fig. 14-b

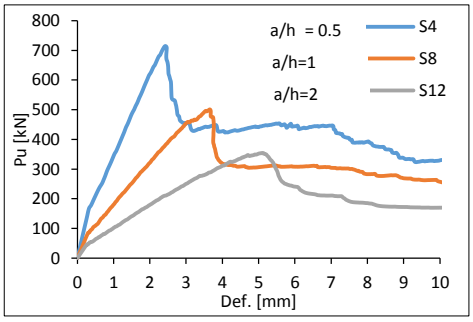

Fig. 14-c

Fig. 14. Effect of shear span-to-depth ratio

A considerable increase with significant enhancement in the toughness (I) which is calculated as the area under the load- deflection curve is observed as a result to an increase of *fc'*. The load deflection curves in Fig.15 expresses how toughness is so significant to an average of 74%. At last, for the crack patterns that are drawn in Fig. 16., It is observed that the raise of (*fc'*) causes to delay the occurrence of premature shear failure for flanged beam.

Fig. 15. Effect of concrete characteristic strength on Deflection

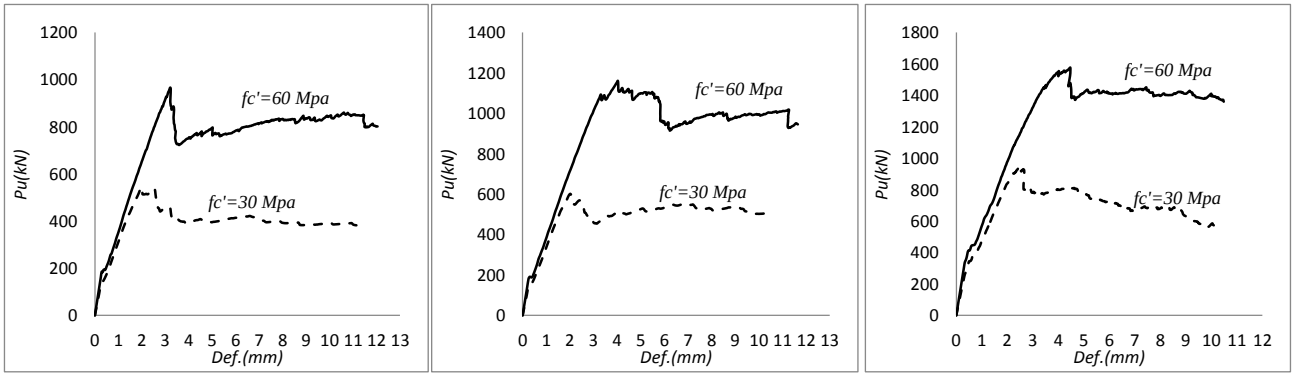

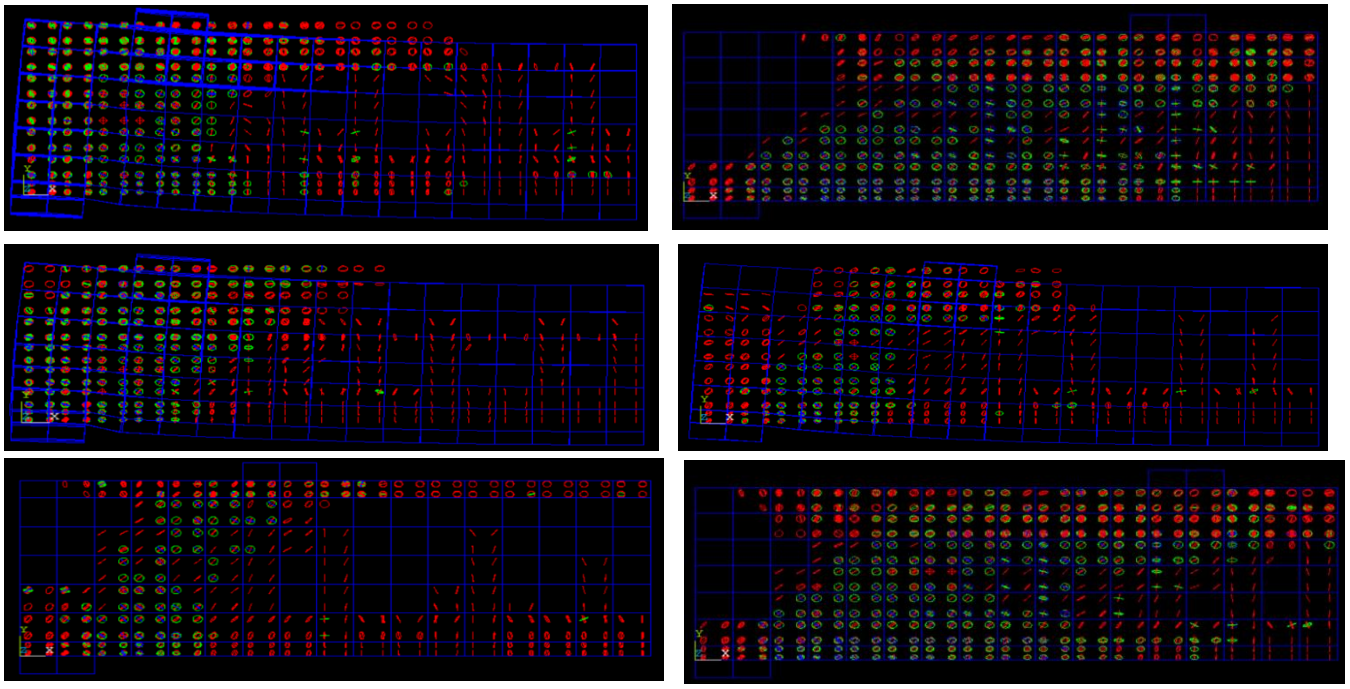

Fig. 16. Crack patterns

5. Conclusions

To sum up from the validation and parametric studies of the finite element computer program ANSYS, the following conclusive points are derived:

[1] A good harmonization in the ending results was achieved by all reached cases of validity, the detected load-deflection response, the points of cracks, and the failure modes which applied the nonlinear FE program (ANSYS). At the final level, the total average value for [$P_{u(FE)}$ / $P_{u(EXP)}$] ratio and [$\Delta_{u(FE)}$ /$\Delta_{u(EXP)}$] ratio for the experimented specimens were 1.03 and 0.87 respectively. This result led us to the use of FE programs.

[2] The most important parameters in this paper were acted by The effectiveness of the ratio of flange width to web width (b_f/b_w) and the ratio of flange depth to web depth (t/h) on the shear strength of a point-loaded reinforced concrete T-beam .To consider the geometric ratios discussed in this theoretical study, it was suggested that the rise in the ratio (b_f/b_w) caused a rise in shear resistance from 12:260%.

[3] The push of longitudinal steel reinforcement ratio (ρ) in the flange from 0.5: 2% of the flange concrete area has helped to enhancement in shear capacity by 14:18% for a/h =0.5, 5:9 % for a/h = 1 and 37:40% for a/h = 2.

References

[1] ANSYS-Release Version 19.2.0., "A Finite Element Computer Software and User Manual for Nonlinear Structural Analysis," ANSYS Inc. Canonsburg, PA 15317, 2018.

[2] Hesham A. A. and Wael M. M., "Shear behavior of reinforced lightweight concrete T-beams, beams," Life Sci J, 16(8), 2019.

[3] Balamuralikrishnan R. and Saravanan J., "Finite Element Modelling of RC T - Beams Reinforced Internally with GFRP Reinforcements," Civil Engineering Journal, 5(3), 2019.
[4] Hamdy K. S., Mohamed M. H., Mahmoud A. K. and Mahmoud Y. A. Z. "Finite Element Analysis on the behavior of Strengthened RC Shallow T-Beams with Large Openings at Shear Zone Using CFRP and BFRP sheets," IJSEAS, 3(11), 2017.
[5] Hugo C. B., Carlos C. and Manuel A.G., "Smeared Crack Analysis of Reinforced Concrete T-Beams Strengthened With Gfrp Composites," Engineering Structures 56, 2013.
[6] Pansuk W and Sato Y., "Shear Mechanism Of Reinforcement Concrete T-Beams With Stirrups," Journal of Advanced Concrete Technology, 5(3), 2007.
[7] Pansuk W., Sato Y., Takahashi R. and Ueda T., "Influence of Top Flange to Shear Capacity of Reinforced Concrete T-Beams," Concrete Engineering Annual Papers, 26(2), 2004.
[8] Giaccio C., Al-Mahaidi R, and Taplin G., "Experimental study on the effect of flange geometry on the shear strength of reinforced concrete T-beams subjected to concentrated loads," Can. J. Civ. Eng. 29,2002
[9] Kachlakev D., and Miller T., "Finite Element Modeling of Reinforced Concrete Structures Strengthened with FRP Laminates," Final Report, Oregon Department of Transportation, Salem, Oregon, May 2001.
[10] Musmar M. A., Rjoub M. I. and Abdel Hadi M. A., "Nonlinear Finite Element Analysis of Shallow Reinforced Concrete Beams Using SOLID65 Element," ARPN Journal of Engineering and Applied Sciences, 9(2), February 2014.
[11] Tjitradi D., Eliatun E. and Taufik S., "3D ANSYS Numerical Modeling of Reinforced Concrete Beam Behavior under Different Collapsed Mechanisms," International Journal of Mechanics and Applications 2017, 7(1): 14-23
[12] Shah, S. P., Swartz, S. E., and Ouyang, C., "Fracture Mechanics of Concrete," John Wiley & Sons, Inc., New York, New York, 1995.
[13] Bangash, M. Y. H., "Concrete and Concrete Structures: Numerical Modeling and Applications," Elsevier Science Publishers Ltd., London, England, 1989.
[14] Gere, J. M. and Timoshenko, S. P.,"Mechanics of Materials," PWS Publishing Company, Boston, Massachusetts, 1997.
[15] Kachlakev, D.I. and McCurry, D., Jr., "Simulated Full Scale Testing of Reinforced Concrete Beams Strengthened with FRP Composites: Experimental Results and Design Model Verification," Oregon Department of Transportation, Salem, Oregon, June 2000
[16] ElAzab I (2021) Behavior of flanged reinforced concrete beams subjected to shear force. PhD. thesis, Benha University, Benha Faculty of Engineering, Benha, Egypt, May 2021.
[17] ACI Committee 318.,"Building Code Requirements for Structural Concrete ACI," vols. 318–14, 2014.